Two-Dimensional Vanadium Carbide (MXene) as Positive Electrode for Sodium-Ion Capacitors

ARTICLE *in* JOURNAL OF PHYSICAL CHEMISTRY LETTERS · JUNE 2015

Impact Factor: 7.46 · DOI: 10.1021/acs.jpclett.5b00868

4 AUTHORS, INCLUDING:

Yohan Dall'Agnese
Paul Sabatier University - Toulouse III
6 PUBLICATIONS **317** CITATIONS
SEE PROFILE

Yury Gogotsi
Drexel University
627 PUBLICATIONS **26,516** CITATIONS
SEE PROFILE

P. Simon
Paul Sabatier University - Toulouse III
157 PUBLICATIONS **17,414** CITATIONS
SEE PROFILE

THE JOURNAL OF PHYSICAL CHEMISTRY Letters

Letter

pubs.acs.org/JPCL

Two-Dimensional Vanadium Carbide (MXene) as Positive Electrode for Sodium-Ion Capacitors

Yohan Dall'Agnese,[†,‡,§] Pierre-Louis Taberna,[†,‡] Yury Gogotsi,[§] and Patrice Simon*[,†,‡]

[†]Université Paul Sabatier, CIRIMAT UMR CNRS 5085, 118 route de Narbonne, 31062 Toulouse, France

[‡]Réseau sur le Stockage Electrochimique de l'Energie (RS2E), FR CNRS 3459, 33 rue Saint Leu, 80039 Amiens Cedex, France

[§]Department of Materials Science and Engineering and A. J. Drexel Nanomaterials Institute, Drexel University, 3141 Chestnut Street, Philadelphia, Pennsylvania 19104, United States

ABSTRACT: Ion capacitors store energy through intercalation of cations into an electrode at a faster rate than in batteries and within a larger potential window. These devices reach a higher energy density compared to electrochemical double layer capacitor. Li-ion capacitors are already produced commercially, but the development of Na-ion capacitors is hindered by lack of materials that would allow fast intercalation of Na-ions. Here we investigated the electrochemical behavior of 2D vanadium carbide, V_2C, from the MXene family. We investigated the mechanism of Na intercalation by XRD and achieved capacitance of ~100 F/g at 0.2 mV/s. We assembled a full cell with hard carbon as negative electrode, a known anode material for Na ion batteries, and achieved capacity of 50 mAh/g with a maximum cell voltage of 3.5 V.

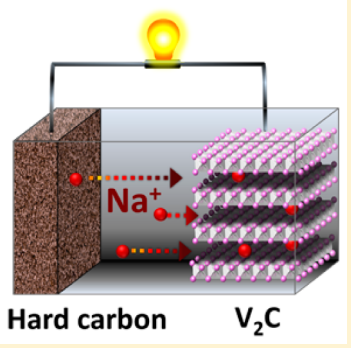

Lithium-ion capacitors (Li-IC) are new promising energy storage devices that bridge the gap between batteries and supercapacitors.[1−3] Because of their high energy and power densities, they are intended for use in a wide variety of applications, such as transportation (electric and hybrid cars), electronics (telephones and laptops), and storage of renewable energy. Ion capacitor materials combine the high energy density from the intercalation mechanism of batteries and the high power of supercapacitor.[4−8] JM Energy and JSR Micro have commercialized a graphite/activated carbon Li-IC; however, the limited supply of lithium and quickly widening use of energy storage devices justify replacement of lithium with cheap and abundant sodium. Sodium ion batteries emerged as an alternative to Li-ion batteries in specific applications, such as large-scale stationary storage, where lower cost can compensate for the lower energy density.[9] Na-ion batteries use hard carbon (HC) as negative electrode with a capacity up to 320 mAh/g at C/10 when cycled in the 2 V window.[10] Similarly to Li-ion batteries, layered metal oxides, such as $NaMnO_2$, $NaCoO_2$, or V_2O_5, have been proposed as positive electrodes, with capacities of 160, 95, and 250 mAh/g, respectively.[11−13]

Recently, sodium-ion capacitors (Na-IC), where the Li intercalation electrode is replaced with a low-cost Na ion electrode,[14] were demonstrated. Most of the ongoing work on these systems is focused on the development of negative electrodes, and several anodes have been proposed, such as carbon nanotubes, $NiCo_2O_4$, and sodium titanate nanotubes.[11−14] In 2012, Kuratani et al. investigated HC/activated carbon Na-IC and showed that HC could be used as negative electrode. Despite Chen et al. proposing V_2O_5, all other studies included activated carbons as positive electrodes,[15,16] and little was done to develop alternative cathodes.

We report the electrochemical characterization of a new positive electrode material, namely, V_2C, that belongs to a large family of 2D transition metal carbides called MXenes.[17] MXenes are synthesized by selective etching of the A layer from MAX phases.[18] Since discovery of the first MXene (Ti_3C_2) in 2011,[19] more than 10 new members have been successfully synthesized and many more predicted. Ti_2C, Ti_3C_2, Nb_2C, and V_2C have quickly drawn the attention as candidates for energy storage due to the possibility of spontaneous intercalation of a variety of cations between their layers.[17−27] For example, Ti_3C_2 has been used in aqueous supercapacitors and as electrode material of Li-, Na-, and K-ion batteries.[25−27] Two layers of Li or Na ions were predicted to intercalate between MXene layers,[27] and the formation of a double-layer of Na has been experimentally shown.[28] From density functional theory (DFT) predictions,[27] V_2C is one of the most promising electrode materials for Li-ion batteries, but experimental results show a very wide working potential window and a sloping charge−discharge;[17,27,29] however, these materials show a potential for assembling hybrid devices, and we previously proposed Ti_2C for Li-ion capacitors.[20] In early 2015, the first experimental investigation of Na-IC using MXenes was published.[28] Wang et al. investigated Ti_2C as negative electrode and alluaudite $Na_2Fe_2(SO_4)_3$ as positive electrode. It showed a good rate capability and high specific power of 1.4 kW/kg with

Received: April 27, 2015
Accepted: June 2, 2015
Published: June 5, 2015

DOI: 10.1021/acs.jpclett.5b00868
J. Phys. Chem. Lett. 2015, 6, 2305−2309

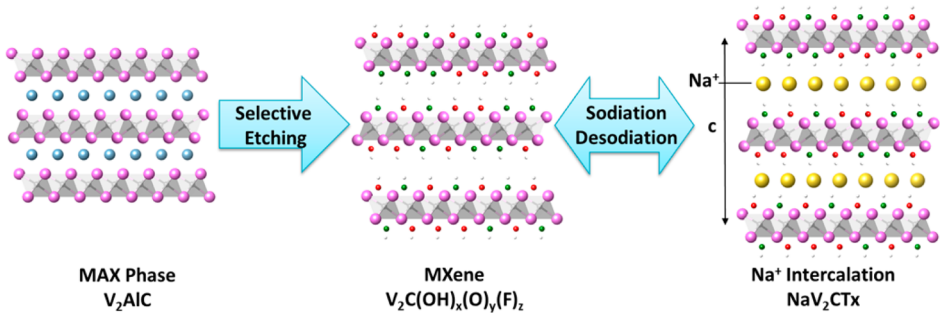

Figure 1. Schematic illustration of the synthesis of V_2CT_x and its sodium intercalation.

specific energy of 260 Wh per kg of Ti_2C. Although promising results were shown, previous sodium ion battery studies demonstrated that Ti_2C is not the best MXene in terms of performance.

To create a Na-IC, we took into account the previous experimental and theoretical research on MXene and selected V_2C as a promising material for Na-IC. In this work, we investigate for the first time the sodiation of V_2C in a half cell. The energy-storage mechanism is studied by X-ray diffraction (XRD) and electrochemical impedance spectroscopy (EIS). To assemble a full cell, we selected HC as negative electrode.

Figure 1 shows a schematic view of the synthesis and structure of V_2C and its Na-intercalation mechanism during cycling. From previous studies,[17,22] it is known that MXenes synthesized using HF contain fluorinated and oxygenated surface functional groups, such as −OH, −O, and −F,[17] and their presence was noted by adding "T_x" to the chemical formula, V_2CT_x. Note that the effect of the surface chemistry has not been studied here.

Figure 2a shows CVs at different scan rates, while the change of the capacitance with the scan rate is described in Figure 2b. High capacitance of 100 F/g or 170 F/cm^3 was obtained at slow scanning, and 50 F/g was still measured at 50 mV/s, evidencing a good power performance of V_2CT_x for Na intercalation. At low scan rates, two different regions can be seen in the CV, corresponding to two different electrochemical processes. From 1 to 2.2 V, the rectangular shape of the CV describes pseudocapacitive behavior. A similar storage mechanism has been previously demonstrated in other MXenes. For example, Ti_3C_2 cycled in aqueous electrolyte exhibits a rectangular-shaped CV attributed to redox reactions and intercalation.[26,30] Redox peaks are identified at low scan rates, with an oxidation peak at 3 V (peak A) and a reduction peak at 2.5 V versus Na^+/Na, (peak B). As the scan rate increases, the redox peaks tend to disappear, thus suggesting a diffusion limitation at scan rate beyond 2 mV/s. The large potential range and the absence of any 2-phase system plateau make V_2C less suitable for sodium ion battery electrodes, but such features are attractive for sodium ion capacitors.

Characterization by EIS was made at different potentials (Figure 3a). The constant charge-transfer resistance, as well as the improvement in the capacitive region at low frequencies, between 1 to 2.5 V correlates well with a pseudocapacitive intercalation mechanism. The charge-transfer resistance (200 Ohm/cm^2) associated with the Na^+ pseudointercalation reaction explains the resistive behavior observed in the CV curves. The increase in the charge-transfer resistance and the semi-infinite diffusion limitation visible in the low-frequency region at 3.2 V is associated with the full desodiation of V_2CTx, in agreement with the redox peaks observed in the CV.

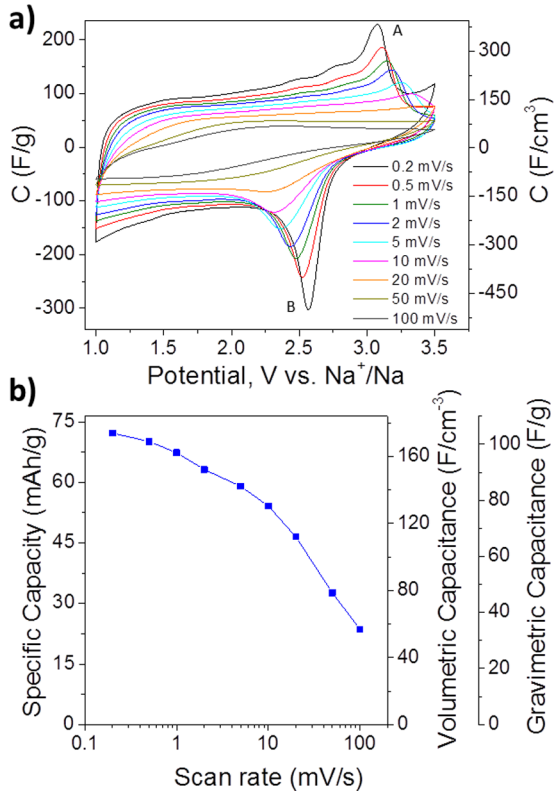

Figure 2. (a) Cyclic voltammetry of V_2CT_x at different scan rate and (b) summary of rate performance.

Figure 3b shows ex situ XRD patterns of V_2CT_x recorded at different voltages, where it can be observed that the (002) peak shifts continuously and reversibly from 9 to 12° during cycling between 1 and 3.5 V versus Na^+/Na. In this potential range, the change is perfectly reversible, thus demonstrating that there are no undesired side reactions. During sodiation, c-lattice parameter increases with the amount of Na^+ stored. This demonstrates that V_2CT_x stores energy through intercalation of Na ions in between layers in a similar way as that previously demonstrated for both intercalation of Li^+ into Ti_2C[20] or Ti_3C_2[31] and Na^+ into Ti_3C_2.[32] There is no new phase appearing at 3.5 V versus Na^+/Na, and thus the redox process identified by peaks A and B in the CV does not modify the crystallographic structure of the material. A 4.6 Å change in c-lattice parameter was observed, as calculated from Bragg's law. Taking into account the fact that there are two interlayer gaps in a lattice unit, there is a 2.3 Å expansion or shrinkage during sodiation and desodiation, respectively. This is a larger change than expected for a single layer of Na^+ ions, which indicates that

DOI: 10.1021/acs.jpclett.5b00868
J. Phys. Chem. Lett. 2015, 6, 2305−2309

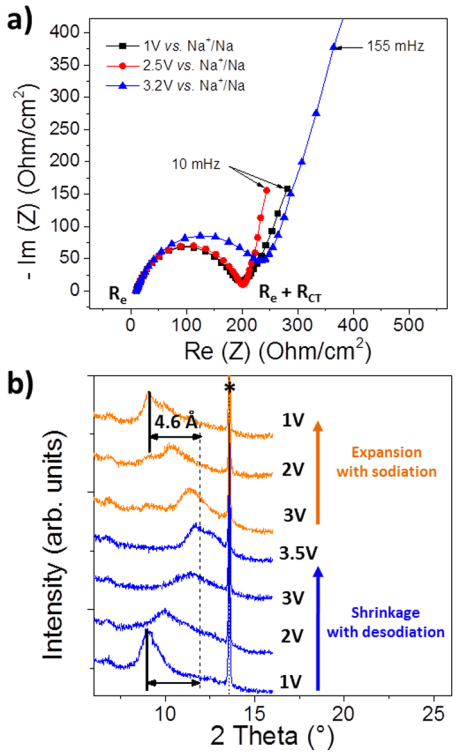

Figure 3. (a) Nyquist plot from EIS. (b) XRD patterns at different potentials. (*) Peak of unreacted V_2AlC.

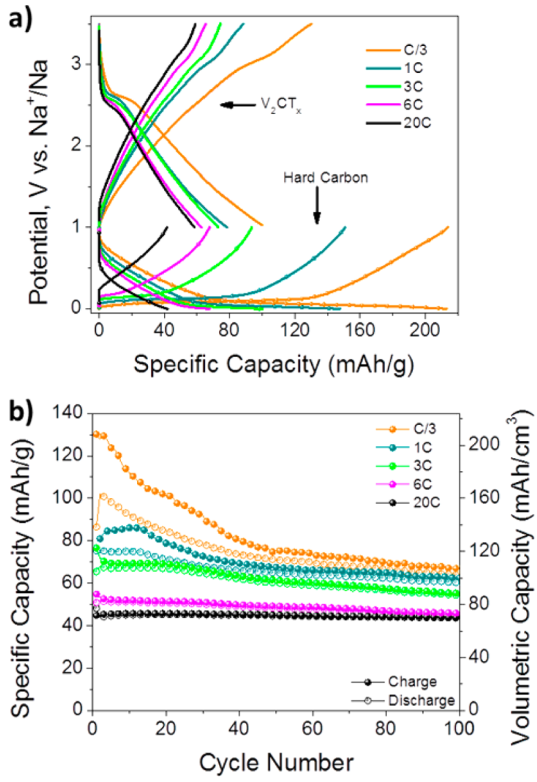

Figure 4. (a) Charge–discharge profiles of V_2CT_x (2 mg) and hard carbon (2 mg) and (b) cycle life from galvanostatic charge–discharge at different rates.

a second layer of Na^+ could be intercalated, as shown for Ti_3C_2 intercalated by Na^+.[32] The peak at 13° corresponds to V_2AlC from incomplete synthesis reaction. This peak does not move during cycling, demonstrating that the MAX phase is not electrochemically active and that the capacity could be increased by increasing V_2CT_x yield. Nevertheless, the presence of this peak is useful as a reference for the other peaks.

Differently from Ti_2C and Ti_3C_2, which can only be used as negative electrodes because of their operating potential window, V_2CT_x shows a potential window ranging from 1 to 3.5 V versus Na^+/Na, being attractive as a positive electrode in Na sodium ion capacitors. V_2CT_x was cycled at current density from 30 mA/g to 1 A/g, corresponding to the rate from C/3 (3 h discharge) to 20C (3 min discharge), as shown in Figure 4b. The objective was to assemble a full cell using V_2CT_x as positive electrode and HC as negative electrode for sodium intercalation.[10] Galvanostatic charge–discharge cycling of HC electrodes was done at the same C rate. The expected key features of a carbon intercalation electrode were observed, with an intercalation potential below 1 V versus Na^+/Na and a capacity beyond 200 mAh/g at low rates (C/3, Figure 4b).

Figure 4b shows the cycling stability at different C-rates. In this example, the positive electrode/negative electrode mass ratio was 1:2, to keep each electrode potential in their working potential window. At low charge/discharge rates, the faradic efficiency decreases, thus leading to a capacity fade with cycling. At low rate (C/3), the capacity fading is more pronounced in the first 40 cycles. Good capacity up to 70 mAh/g was obtained, with remarkable stability at discharge rates beyond 3C. The performance achieved experimentally is lower than that predicted by first-principles simulation corresponding to the maximum theoretical capacity for a bare V_2C monolayer (335 mAh/g).[27] Experimentally, the capacity is limited by the presence of MAX phase residue, functionalized layers, and stacked layers. Thus, there is much room for further increase in capacitance of this material.

On the basis of half-cell results, hybrid Na-ion capacitor cells were assembled. By anticipating the capacity decrease in V_2CT_x during the first cycles, we calculated a HC/V_2CT_x weight ratio of 1:2. In such conditions, the overcapacitive HC electrode allows a better potential stability for the negative electrode. Before assembling a full cell, each electrode was pretreated as described in the Experimental Methods. The full cells were tested from C/3 to 20C rate. Figure 5 shows the electrochemical performance obtained in a full cell configuration. All gravimetric capacities are calculated based on the total weight of both positive and negative electrodes to focus on the performances of the device. Because the mass ratio of positive to negative electrode is 1:2, the equivalent capacities based on the mass of V_2CT_x are three times higher than those presented in Figure 5.

The charge/discharge galvanostatic profiles are presented in Figure 5a. During discharge, a sharp potential drop occurred from 3.5 V down to 2.6 V, followed by a small plateau at 2.5 V due to the redox reaction peaks observed in Figure 2a, so that the practical cell voltage was 2.6 V. Figure 5b shows that high-power performance could be achieved, with 40% of the total capacity obtained at 20C, despite the use of a Na-ion intercalation HC negative electrode. The capacity decrease during the first cycles at the low rate (C/3) is associated with a decrease in the Coulombic efficiency due to redox reaction beyond 3 V.

Figure 5c shows the cycle life of the full cell at a high rate (20C). After 300 cycles, the capacity retention was 70%. Interestingly, the capacity slightly increased during the first 70 cycles. Afterward, the capacity decrease was associated with the

DOI: 10.1021/acs.jpclett.5b00868
J. Phys. Chem. Lett. 2015, 6, 2305–2309

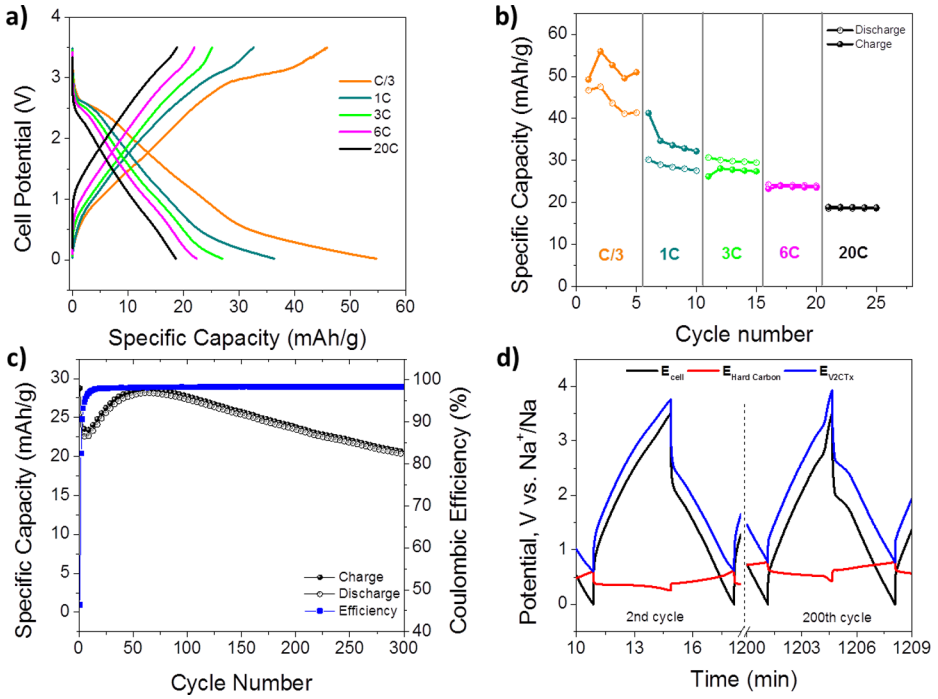

Figure 5. (a) Charge−discharge profiles at various rates. (b) Change of the capacity during galvanostatic charge−discharge at different rates. (c) Capacity versus cycle number. (d) Details of the potential range of positive and negative electrodes at 1A/g. Capacities were calculated for the total mass of both positive and negative active material, taken in the weight ratio of 1:2.

decrease in the faradic efficiency down to 98%. To better understand this decrease, both electrodes were studied using a three-electrode cell. Figure 5d shows the 2nd and 200th cycles. First, we can notice that the negative electrode potential range is smaller than 1 V because HC is in excess. As previously explained, a slightly overcapacitive negative electrode is necessary to ensure a good stability. Although the positive electrode has low irreversibility, it is sufficient to drive a shift of the negative electrode toward higher potentials after a large number of cycles. The potential of the V_2CT_x electrode goes slightly beyond the optimum operating potential range of 1 to 3.5 V, which leads to irreversible redox reactions, thus explaining the capacity decrease upon cycling. An optimization of the electrode mass ratio should prevent the observed drift of the positive electrode potential, leading to an improvement in cyclability.

It is important to note that all results shown here were obtained on samples containing residual MAX phase and therefore decreased the overall performances. Recently, another synthesis route of MXene, via a fluoride salt and HCl etching, was proposed,[33] and samples produced by that method showed improved capacitance. It may offer material of higher purity, which will also show improved performance in Na-ion capacitors. Finally, with just two MXenes studied in Na-ion capacitors to date and already showing promise for use as both negative and positive electrodes, there is clear opportunity to create devices with both electrodes made of 2D carbides, but further studies of electrochemical behavior of those new materials are needed.

This work shows that at least one representative of the large family of MXenes, V_2CT_x, can serve as the positive electrode for a sodium ion capacitor. Investigation of the mechanism of sodiation and desodiation of V_2CT_x by XRD shows continuous intercalation of sodium ions between the V_2CT_x layers in a wide range of potentials. Electrochemical testing in half cells demonstrated that both capacitive (pseudocapacitive) and diffusion-limited redox processes take place. An asymmetric full cell was assembled using hard carbon, a known anode material for sodium ion battery. V_2CT_x/HC sodium-ion capacitor showed promising results, with a maximum cell voltage of 3.5 V and a capacity of 50 mAh/g.

EXPERIMENTAL METHODS

V_2C was synthesized by selectively etching the aluminum layer out of the MAX phase V_2AlC with a 50% concentrated HF solution for 8h. Hard carbon was synthesized by pyrolysis of sugar under argon flow, as described elsewhere.[10]

XRD patterns of the V_2CT_x electrodes were collected using a Bruker D4 diffractometer using a Cu Kα radiation (λ = 1.5406 Å) in the range 2θ = 5−50° with a step of 0.016°. The samples were polarized and maintained at a given potential versus metallic sodium in a Swagelok cell prior to testing.

The electrodes were rolled and cut into ∼30 μm thick disks with average mass loading of 5 mg·cm^{-2}. V_2CT_x electrodes were prepared with 5 wt % polytetrafluoroethylene binder (60 wt % in H_2O, Aldrich) and 15 wt % carbon black (Alfa Aesar) to secure a sufficient electronic conductivity. Hard carbon electrodes were prepared with 5 wt % polytetrafluoroethylene binder (60 wt % in H_2O, Aldrich).

A two-electrode Swagelok cell was used for half-cells with metallic sodium as counter and reference electrode separated by a glass fiber separator (GFA). Full cells were assembled in three-electrode Swagelok cells using an Ag wire as pseudoreference electrode. The electrodes were presodiated by immersing them in the electrolyte and short-circuited with metallic sodium. The electrolyte used was 1 M $NaPF_6$ in EC/DMC (1:1). The cells were assembled in an argon-filled glovebox.

A VMP3 potentiostat (Biologic SA, France) was used for electrochemical testing by cyclic voltammetry (CV), galvano-

DOI: 10.1021/acs.jpclett.5b00868
J. Phys. Chem. Lett. 2015, 6, 2305−2309

static charge−discharge, and electrochemical impedance spectroscopy (EIS). In full cells, capacities were calculated based on the total masses of negative and positive electrodes.

AUTHOR INFORMATION

Corresponding Author

*E-mail: simon@chimie.ups-tlse.fr. Tel: +33(0)5.61.55.68.02.

Notes

The authors declare no competing financial interest.

ACKNOWLEDGMENTS

We thank B. Anasori for help with V_2AlC synthesis. This work was supported by the Partner University Fund (PUF) of French Embassy. Y.D.A. was supported by the European Research Council (ERC, Advanced Grant, ERC-2011-AdG, Project 291543 − IONACES). P.S. acknowledges funding from the Chair of Excellence of the Airbus group foundation "Embedded multi-functional materials". Y.G. was partially supported by the Competitive Research Grant from King Abdullah University for Science & Technology (KAUST).

REFERENCES

(1) Dubal, D. P.; Ayyad, O.; Ruiz, V.; Gomez-Romero, P. Hybrid Energy Storage: The Merging of Battery and Supercapacitor Chemistries. *Chem. Soc. Rev.* **2015**, *44*, 1777−1790.

(2) Armand, M.; Tarascon, J. M. Building Better Batteries. *Nature* **2008**, *451*, 652−657.

(3) Cericola, D.; Kötz, R. Hybridization of Rechargeable Batteries and Electrochemical Capacitors: Principles and Limits. *Electrochim. Acta* **2012**, *72*, 1−17.

(4) Naoi, K.; Ishimoto, S.; Miyamoto, J.-i.; Naoi, W. Second Generation 'Nanohybrid Supercapacitor': Evolution of Capacitive Energy Storage Devices. *Energy Environ. Sci.* **2012**, *5*, 9363−9373.

(5) Amatucci, G. G.; Badway, F.; Du Pasquier, A.; Zheng, T. An Asymmetric Hybrid Nonaqueous Energy Storage Cell. *J. Electrochem. Soc.* **2001**, *148*, A930−A939.

(6) Du Pasquier, A.; Plitz, I.; Menocal, S.; Amatucci, G. A Comparative Study of Li-Ion Battery, Supercapacitor and Nonaqueous Asymmetric Hybrid Devices for Automotive Applications. *J. Power Sources* **2003**, *115*, 171−178.

(7) Khomenko, V.; Raymundo-Piñero, E.; Béguin, F. High-Energy Density Graphite/AC Capacitor in Organic Electrolyte. *J. Power Sources* **2008**, *177*, 643−651.

(8) Naoi, K.; Simon, P. New Materials and New Configurations for Advanced Electrochemical Capacitors. *J. Electrochem. Soc.* **2008**, *17*, 34−37.

(9) Slater, M. D.; Kim, D.; Lee, E.; Johnson, C. S. Sodium-Ion Batteries. *Adv. Funct. Mater.* **2013**, *23*, 947−958.

(10) Ponrouch, A.; Goñi, A. R.; Palacín, M. R. High Capacity Hard Carbon Anodes for Sodium Ion Batteries in Additive Free Electrolyte. *Electrochem. Commun.* **2013**, *27*, 85−88.

(11) Aravindan, V.; Gnanaraj, J.; Lee, Y.-S.; Madhavi, S. Insertion-Type Electrodes for Nonaqueous Li-Ion Capacitors. *Chem. Rev.* **2014**, *114*, 11619−11635.

(12) Zhang, Y.; Yuan, C.; Ye, K.; Jiang, X.; Yin, J.; Wang, G.; Cao, D. An Aqueous Capacitor Battery Hybrid Device Based on Na-Ion Insertion-Deinsertion in λ-MnO_2 Positive Electrode. *Electrochim. Acta* **2014**, *148*, 237−243.

(13) Kuratani, K.; Yao, M.; Senoh, H.; Takeichi, N.; Sakai, T.; Kiyobayashi, T. Na-Ion Capacitor Using Sodium Pre-Doped Hard Carbon and Activated Carbon. *Electrochim. Acta* **2012**, *76*, 320−325.

(14) Ding, R.; Qi, L.; Wang, H. An Investigation of Spinel $NiCo_2O_4$ as Anode for Na-Ion Capacitors. *Electrochim. Acta* **2013**, *114*, 726−735.

(15) Chen, Z.; Augustyn, V.; Jia, X.; Xiao, Q.; Dunn, B.; Lu, Y. High-Performance Sodium-Ion Pseudocapacitors Based on Hierarchically Porous Nanowire Composites. *ACS Nano* **2012**, *6*, 4319−4327.

(16) Yin, J.; Qi, L.; Wang, H. Sodium Titanate Nanotubes as Negative Electrode Materials for Sodium-Ion Capacitors. *ACS Appl. Mater. Interfaces* **2012**, *4*, 2762−2768.

(17) Naguib, M.; Halim, J.; Lu, J.; Cook, K. M.; Hultman, L.; Gogotsi, Y.; Barsoum, M. W. New Two-Dimensional Niobium and Vanadium Carbides as Promising Materials for Li-Ion Batteries. *J. Am. Chem. Soc.* **2013**, *135*, 15966−15969.

(18) Naguib, M.; Gogotsi, Y. Synthesis of Two-Dimensional Materials by Selective Extraction. *Acc. Chem. Res.* **2015**, *48*, 128−135.

(19) Naguib, M.; Kurtoglu, M.; Presser, V.; Lu, J.; Niu, J.; Heon, M.; Hultman, L.; Gogotsi, Y.; Barsoum, M. W. Two-Dimensional Nanocrystals Produced by Exfoliation of Ti_3AlC_2. *Adv. Mater.* **2011**, *23*, 4248−4253.

(20) Come, J.; Naguib, M.; Rozier, P.; Barsoum, M. W.; Gogotsi, Y.; Taberna, P. L.; Morcrette, M.; Simon, P. A Non-Aqueous Asymmetric Cell with a Ti_2C-Based Two-Dimensional Negative Electrode. *J. Electrochem. Soc.* **2012**, *159*, A1368−A1373.

(21) Hu, Q.; Sun, D.; Wu, Q.; Wang, H.; Wang, L.; Liu, B.; Zhou, A.; He, J. MXene: A New Family of Promising Hydrogen Storage Medium. *J. Phys. Chem. A* **2013**, *117*, 14253−14260.

(22) Dall'Agnese, Y.; Lukatskaya, M. R.; Cook, K. M.; Taberna, P.-L.; Gogotsi, Y.; Simon, P. High Capacitance of Surface-Modified 2D Titanium Carbide in Acidic Electrolyte. *Electrochem. Commun.* **2014**, *48*, 118−122.

(23) Yan, P.; Zhang, R.; Jia, J.; Wu, C.; Zhou, A.; Xu, J.; Zhang, X. Enhanced Supercapacitive Performance of Delaminated Two-Dimensional Titanium Carbide/Carbon Nanotube Composites in Alkaline Electrolyte. *J. Power Sources* **2015**, *284*, 38−43.

(24) Liang, X.; Garsuch, A.; Nazar, L. F. Sulfur Cathodes Based on Conductive Mxene Nanosheets for High-Performance Lithium−Sulfur Batteries. *Angew. Chem.* **2015**, *127*, 3979−3983.

(25) Mashtalir, O.; Naguib, M.; Mochalin, V. N.; Dall'Agnese, Y.; Heon, M.; Barsoum, M. W.; Gogotsi, Y. Intercalation and Delamination of Layered Carbides and Carbonitrides. *Nat. Commun.* **2013**, *4*, 1716.

(26) Lukatskaya, M. R.; Mashtalir, O.; Ren, C. E.; Dall'Agnese, Y.; Rozier, P.; Taberna, P. L.; Naguib, M.; Simon, P.; Barsoum, M. W.; Gogotsi, Y. Cation Intercalation and High Volumetric Capacitance of Two-Dimensional Titanium Carbide. *Science* **2013**, *341*, 1502−1505.

(27) Xie, Y.; Dall'Agnese, Y.; Naguib, M.; Gogotsi, Y.; Barsoum, M. W.; Zhuang, H. L.; Kent, P. R. C. Prediction and Characterization of Mxene Nanosheet Anodes for Non-Lithium-Ion Batteries. *ACS Nano* **2014**, *8*, 9606−9615.

(28) Wang, X.; Kajiyama, S.; Iinuma, H.; Hosono, E.; Oro, S.; Moriguchi, I.; Okubo, M.; Yamada, A. Pseudocapacitance of MXene Nanosheets for High-Power Sodium-Ion Hybrid Capacitors. *Nat. Commun.* **2015**, *6*, 6544.

(29) Ji, X.; Xu, K.; Chen, C.; Zhang, B.; Wan, H.; Ruan, Y.; Miao, L.; Jiang, J. Different Charge-Storage Mechanisms in Disulfide Vanadium and Vanadium Carbide Monolayer. *J. Mater. Chem. A* **2015**, *3*, 9909−9914.

(30) Lukatskaya, M. R.; Bak, S.-M.; Yu, X.; Yang, X.-Q.; Barsoum, M. W.; Gogotsi, Y. Probing the Mechanism of High Capacitance in 2D Titanium Carbide Using in Situ X-Ray Absorption Spectroscopy. *Adv. Energy Mater.* **2015**, DOI: 10.1002/aenm.201500589.

(31) Xie, Y.; Naguib, M.; Mochalin, V. N.; Barsoum, M. W.; Gogotsi, Y.; Yu, X.; Nam, K.-W.; Yang, X.-Q.; Kolesnikov, A. I.; Kent, P. R. C. Role of Surface Structure on Li-Ion Energy Storage Capacity of Two-Dimensional Transition-Metal Carbides. *J. Am. Chem. Soc.* **2014**, *136*, 6385−6394.

(32) Wang, X.; Shen, X.; Gao, Y.; Wang, Z.; Yu, R.; Chen, L. Atomic-Scale Recognition of Surface Structure and Intercalation Mechanism of Ti_3C_2X. *J. Am. Chem. Soc.* **2015**, *137*, 2715−2721.

(33) Ghidiu, M.; Lukatskaya, M. R.; Zhao, M.-Q.; Gogotsi, Y.; Barsoum, M. W. Conductive Two-Dimensional Titanium Carbide 'Clay' with High Volumetric Capacitance. *Nature* **2014**, *516*, 78−81.

DOI: 10.1021/acs.jpclett.5b00868
J. Phys. Chem. Lett. 2015, 6, 2305−2309